Filtering of electron images of crystal defects

J. Desseaux, C. d'Anterroches, J.M. Penisson, A. Renault

Classification
Physics Abstracts
07.80 — 42.30

Filtering of electron images of crystal defects

J. Desseaux, C. d'Anterroches, J. M. Penisson and A. Renault

Section Physique du Solide/DRF, 85 X, 38041 Grenoble Cedex, France

(*Reçu le 1er octobre 1979, révisé le 24 janvier, accepté le 15 février 1980*)

Résumé. — Pour rendre l'interprétation des images obtenues au microscope électronique plus aisée, il est nécessaire de filtrer le bruit photographique et électronique. Le filtrage peut être soit optique soit numérique. Cependant l'utilisation des masques ne doit pas perturber le spectre de Fourier du signal au point d'altérer l'image des défauts cristallins observés. On présente diverses formes de masque et leur influence sur la restitution de l'image d'objets tests. Enfin un filtrage numérique est appliqué à une image de colonnes atomiques autour d'une dislocation obtenue réellement au microscope électronique.

Abstract. — The interpretation of electron micrographs becomes easier after filtering of the photographic and electronic noise. The filtering process can be optical or numerical. The use of mask in the Fourier space must not disturb too much the spectrum of the information of interest. The influence of four mask shapes is studied on two nearly similar test objects : atomic columns near the core of germanium crystal dislocations. The optimal mask shape is applied to a real electron micrograph of a high resolution electron image of dislocation.

1. **Introduction.** — Interpretation of high resolution electron micrographs of crystal defects consists of extraction of structural information about the specimen. Generally this interpretation is blurred by noise and it is often necessary to increase the signal to noise ratio of the image. The methods for enhancing it are generally based on Fourier analysis : they may be analogue (optical) or digital methods. All these methods are appropriate and have been widely applied to periodic objects.

These methods perform the Fourier transform (optics) or the Fourier series (numerical methods) of the signal. The spatial frequencies of interest are then selected by a suitable filter and the image is then restored by an inverse Fourier transform. For electron micrographs of crystals at atomic scale the filter used is generally a binary optical or numerical mask. For filtering of periodic objects the holes must be as small as possible. But this cannot be done for non periodic objects where we know that the information is not concentrated at particular spatial frequencies.

The noise due to electronic and photographic processes in the micrograph is superimposed on the signal and it is necessary to know its spectrum to restore the image. The noise due to photographic films can be considered as additive and does not depend on the signal and has a flat spectrum [1, 2]. Then the reconstruction will be much more affected when the spectrum of the noise and that of the signal are in the same frequency range and of the same order of magnitude.

Our goal is to filter 500 kV electron micrographs. In this case the transfer function of the electron microscope has no sign reversals down to 0.3 $Å^{-1}$. Spatial optical zonal filtering [3] or numerical treatment of the transfer function is not necessary.

We are concerned here neither with image formation in the microscope nor with electron matter interaction. However we must keep them in mind for ultimate interpretation of micrographs.

Our purpose is to study the structure of dislocation cores in crystals whose atomic columns have been imaged with high resolution electron microscope [4, 5]. In this paper we want to test the influence of different mask shapes on the reconstruction of the image of two slightly different objects : the calculated atomic positions around two almost similar dislocation cores [6]. The optical method of filtering will be described in detail. Computer simulations of the filtering of the same objects have also been performed. The comparison is made between optical and numerical filterings. The test objects are without noise. Finally the real case of numerical filtering of a noisy electron micrograph of a dislocation is presented.

2. **Optical analysis and image reconstruction.** — The optical spatial analysis of an image is based on the ability of a lens to perform a two-dimensional Fourier transform of an object coherently illuminated. A coherent optical process of filtering and reconstruction was first proposed by Maréchal and Croce [7].

Klug and Berger [8] used for the first time the optical Fourier analysis of electron micrographs to study biological periodic structures, but they only recorded the Fraunhofer diffraction pattern in the squared modulus of the Fourier transform. The subsequent step of optical processing is to manipulate the spatial frequency spectrum with suitably chosen filters to restore enhanced images as done by Klug and de Rosier [9]. This permitted them to improve the signal to noise ratio and to separate twosided images of virus. This coherent optical process has been completely described by O'Neil [10] and widely developed for example by Van der Lugt [11] or Goodman [12].

2.1 FOURIER ANALYSIS. — The lens arrangement we use, for optical filtering is shown schematically in figure 1.

A coherent point source is placed on the optical axis in the (x_0, y_0) plane.

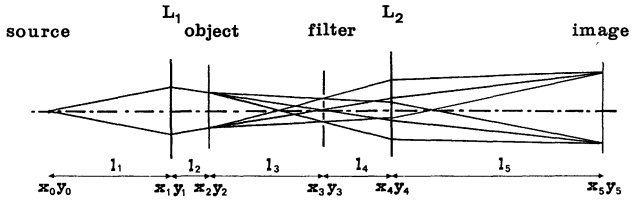

Fig. 1. — Lens arrangement used for optical filtering.

The lens L_1 of focal length f_1 is at a distance l_1 from the source. Its effect is to modify the incident amplitude by a multiplicative phase factor [12]. The object modifies the amplitude by a transmission function $f(x_2, y_2)$. The resulting wave amplitude distribution in a plane situated at a distance l_3 from the object is proportional to the Fourier transform of the illuminated object : $O(u, v)$. The intensity distribution recorded on a film situated at l_3 is

$$I(x_3, y_3) = \left| A.O\left(\frac{x_3}{\lambda l_3}, \frac{y_3}{\lambda l_3}\right)\right|^2$$

A is a complex factor which does not depend on x_3 and y_3, λ is the wavelength. It must be noted that with the lens arrangement used (the objects is situated behind the lens L_1) the magnification of the diffraction pattern depends only on l_3 and the position of the diagram does not depend on the position of the object. It is a great utility for the experimentator.

2.2 IMAGE RECONSTRUCTION. — In the Fourier plane (x_3, y_3) we introduce a filter

$$F\left(\frac{x_3}{\lambda l_3}, \frac{y_3}{\lambda l_3}\right)$$

which acts only on the amplitude.

The image is reconstructed by a lens L_2 (Fig. 1) of focal length f_2 situated at a distance l_4 from the Fourier plane. If the geometrical condition of imaging is fulfilled

$$\frac{1}{l_3 + l_4} + \frac{1}{l_5} = \frac{1}{f_2}$$

the wave amplitude, in the plane $(x_5\, Oy_5)$ at l_5 behind the lens L_2, is proportional to the convolution product of the object with the inverse Fourier transform $f(x)$ of the filter F. The recorded intensity distribution is given by :

$$I(x_5, y_5) = \left| B.O(x_5, y_5) * f\left(-\frac{x_5}{M_2}, -\frac{y_5}{M_2}\right)\right|^2$$

$*$ is the convolution product ; M_2 is the magnification of the lens L_2. B is a complex factor which does not depend on x_5 and y_5.

The reconstructed image is inverted with respect to the object.

If the filter is equal to unity throughout the whole spatial frequency band of the object and if the lens L_2 aperture is sufficiently large, then $I(x_5, y_5)$ is directly proportional to the intensity transmittance of the object. Otherwise the L_2 aperture limites the resolution in the reconstructed image.

3. **Experimental methods.** — 3.1 TEST OBJECTS. — We have to test the validity of simple binary filtering. Thus we have constructed test objects which look like the objects we observe with the electron microscope i.e. dislocations in crystal [5]. The test objects are the calculated atomic positions around two similar dislocation cores. The dislocation is a pure edge dislocation along the [011] direction with a Burgers vector $1/2\,[0\bar{1}1]$ in a germanium crystal (cubic diamond structure) oriented [011]. One dislocation core is empty (Fig. 2*a*), the other contains a supplementary atomic column (Fig. 2*b*). The atomic positions are calculated with the isotropic elastic theory, as given by Hirth and Lothe [13]. The goal of the filtering of these test objects is to search for the most suitable shape of the mask which will remove the greatest part of the noise without altering the information about a possible supplementary column in the core.

3.2 THE COHERENT OPTICAL BENCH. — The coherent source is a laser. A spherical wave given by a highly divergent lens falls on the first lens L_1 (Fig. 1) whose focal length is 750 mm. The focal length of the lens L_2 is 700 mm. Both lens are well corrected and cleaned.

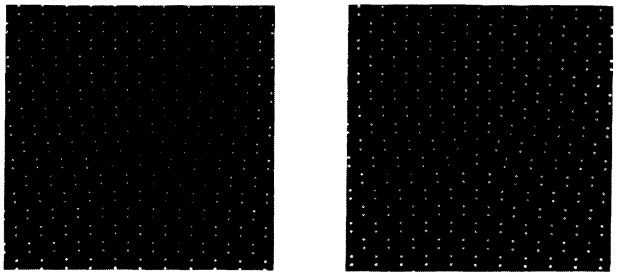

a) *b)*

Fig. 2. — The two test objects : edge dislocation cores in Ge [011] : *a*) one is empty ; *b*) the other contains a supplementary atomic column.

The alignment of the optical axis must be accurate. The test objects are reprinted on photographic film 6.5 × 9 mm. The magnification of the object with respect to the real germanium crystal is about 10^7. The diffraction pattern and the reconstructed images are recorded on photographic film ILFORD FP4 developed with ID11. The total length of the optical bench is about 4.5 m.

3.3 OPTICAL MASK MAKING. — The masks used are only opaque screens with holes suitably placed. The beams diffracted outside the holes are cut off and do not contribute to the image. Accurate masks are made with a photographic etching process.

The optical diffractogram of the object (Fig. 3) is recorded and enlarged to locate accurately the diffraction spots. At this stage the shape of the holes must be chosen. We must take into account that our objects are not exactly periodic. Therefore the representative spatial frequency bands are extended around the reciprocal lattice points. With this in mind, we draw different hole shapes around the spots of interest.

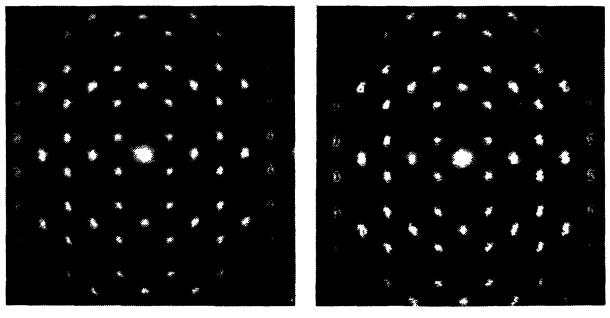

a) *b)*

Fig. 3. — The optical diffractogram of the objects respectively 2*a* and 2*b*.

3.4 CHOICE OF OPTICAL MASK SHAPE. — The 100 kV electron microscope has a resolution of 2.5 to 3 Å (i.e. 0.33 $Å^{-1}$ to 0.4 $Å^{-1}$). Apart from the sign reversals of the transfer function the Ge lattice images are obtained by the interference of the four 111 beams with the 000 non diffracted beam [16]. In the case of a 500 kV electron microscope the resolution reaches 3 Å without any transfer function sign reversal. The lattice fringes are obtained with the same beams [17]. Thus we just consider the four 111 spots and the 000 spot to restore the image from the optical diffractogram.

We have tested three types of mask shapes.

1) *Type* 1 : a disc mask (Fig. 4*a*) with a cut-off spatial frequency of $\frac{11}{8}\, g_{111} = 0.5$ $Å^{-1}$ which corresponds to the limit of resolution of the 500 kV electron microscope. This aperture is similar to the one used in the electron microscopes. Apart from electron microscope aberrations and dynamical interaction we are imitating electron microscope imaging conditions.

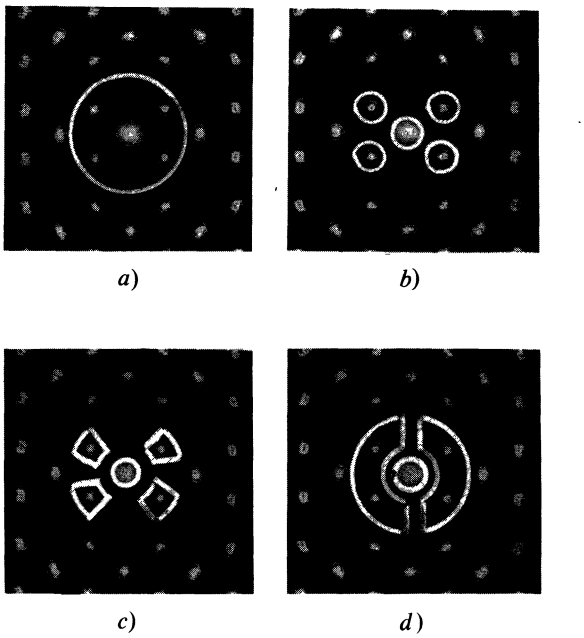

a) *b)* *c)* *d)*

Fig. 4. — Mask shapes : *a*) disc mask with a cut off frequency $g_c = \frac{11}{8}\, g_{111}$; *b*) mask with round holes of radius $g_F = g_{111}/4$; *c*) mask with special holes shape taking into account the angular (± 5°) and the parameter (± 20 %) distortion of the atomic planes around the core ; *d*) semi annular mask.

2) *Type* 2 : a mask with holes just permitting the five spots 111 and 000 and their immediate surrounding to contribute to the image.

In fact the information seems to be limited to just around the fundamental diffracted beams (Fig. 3). And intuitively with such shapes the greatest part of the noise can be removed. We have tested two different hole shapes. Figure 4*b* shows round holes (diameter $g_{111}/2$). In figure 4*c* the holes are asymmetric to take into account the angular distortion of the atomic planes near the dislocation core (± 5°) and the interatomic distortion ($\Delta g/g = \pm$ 20 %).

3) *Type* 3 : an almost annular mask permitting a larger spatial frequency band to contribute to the image side removing the low spatial frequency noise ($< g_{111}/2$) due to contamination and high spatial frequency noise ($> \frac{11}{8} g_{111}$) due to photographic or electronic process (Fig. 4*d*).

4. **Experimental results of optical filtering.** — 4.1 DIFFRACTION DIAGRAMS. — Figure 3 shows the optical diffractogram of the test objects. No difference is visible between the diffractograms of the two types of dislocation cores. The diagram of a cubic diamond structure oriented [011] is recognizable on both of them but the spots are extended around each reciprocal lattice point which corresponds to the perfect crystal. It must be noted that the intensity distribution is similar to the one found by Willis [18] for an optical diffraction diagram of an edge dislocation in a simple cubic structure. The information about the dislocation seems to be concentrated just around the perfect crystal diffraction spots. This point will be discussed when we have to choose the optimal mask shape.

4.2 RECONSTRUCTED IMAGES. — We have tested the influence of the three types of masks on the reconstruction of the two almost similar dislocation cores. Our experimental conclusions are as follows (Fig. 5) :

i) For all reconstructed images the two atomic columns 1.4 Å apart, are not separated, due to the cut off frequency in all masks which does not permit the (004) spot to contribute to image formation.

ii) For all images, the regions which correspond to the perfect crystal are well reconstructed. The intensity maxima are on the projection of the atomic columns. The fundamental spatial frequency is faithfully restored. But in these perfect regions subsidiary weak peaks between the fundamental peaks can be seen. This is due to the fact that in the optical diffractogram the 111 spots have a non negligible intensity with respect to the 000 spot. The original prints have a high contrast (Fig. 2). Thus in the reconstructed image intensity distribution, the term which corresponds to twice the fundamental spatial frequency ($1/3.26$ Å^{-1}) is visible. It gives some intensity between the fundamental periodicity of the crystal.

On the other hand, if the original object has a low contrast (as is the case with highly magnified electron micrographs) it may be necessary to attenuate the 000 spot of the diffractogram, to enhance the contrast on the reconstructed image. Care must be taken since any partially transmitting screen will introduce phase error. In any case the attenuation of the central spot must not be too great because of the doubling mentioned above.

iii) The image of the dislocation cores is greatly affected by the shape of the mask. In the case where five holes are used the core structure is unrecognizable

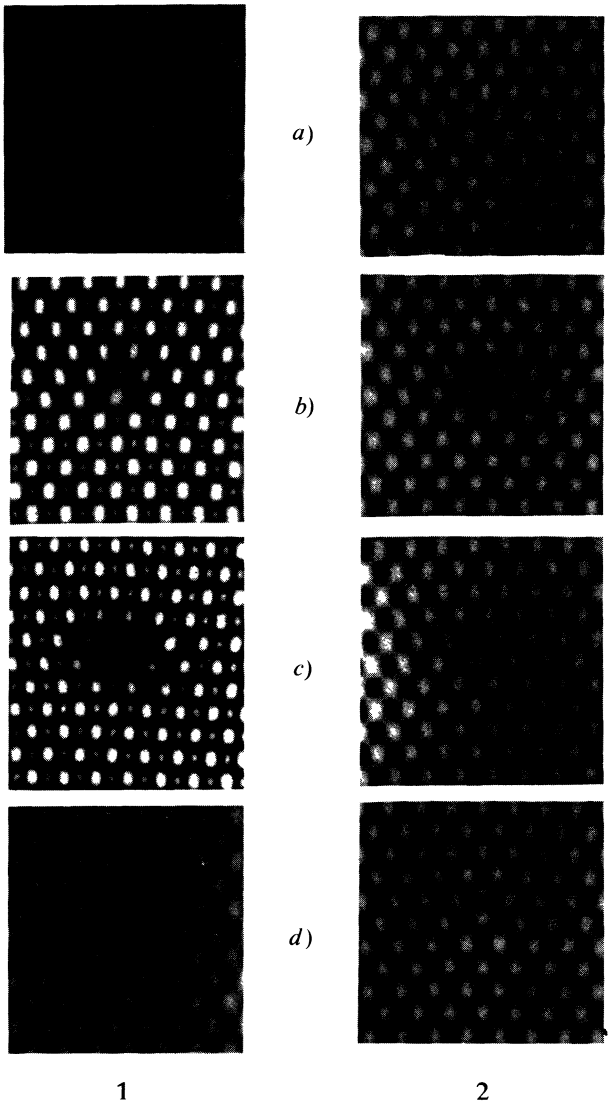

Fig. 5. — Optical simulation of the reconstruction of the two test objects filtered respectively with the four masks shown figures 4*a*, 4*b*, 4*c*, 4*d*. (1) Reconstructed image of the test object 2 *a* ; (2) of the test object 2 *b*.

(Fig. 5*b*, *c*). It is impossible to distinguish if there is an extra atomic column or not. The exact shape of the holes has no influence. The core structure remains blurred even if the special shape filter (Fig. 5*c*) is used. But in the cases, where a disc (Fig. 5*a*) or a ring (Fig. 5*d*) are used the information about details of the cores structures is not entirely lost.

The explanation is the following one (in one dimension for simplicity) : the reconstructed image of the core is the square modulus of the convolution product of the object with the inverse Fourier transform of the mask. A filter, composed of three windows of width $2\, g_F$ around the spatial frequencies $-\, g_{111}$, and $+\, g_{111}$, can be written

$$F(f) = H(f) * [\delta(f - g_{111}) + \delta(f) + \delta(f + g_{111})]$$

where $H(f)$ is the window :

$$H(f) = +1 \quad \text{in the windows}$$
$$H(f) = 0 \quad \text{elsewhere .}$$

The inverse Fourier transform of such a mask is

$$f(x) = h(x).[1 + 2\cos 2\pi g_{111}\, x]$$

where $h(x)$ is the inverse Fourier transform of $H(f)$,

$$h(x) = 2\, g_F \frac{\sin 2\pi g_F\, x}{2\pi g_F\, x} \quad \text{with} \quad g_F = \frac{g_{111}}{4}.$$

Thus the amplitude of $f(x)$ is sketched figure 6*a*. The final reconstructed image is the square modulus of the convolution product of $h(x)$ with the object distribution. We see that there is an enhancement of the fundamental periodicity $1/g_{111}$.

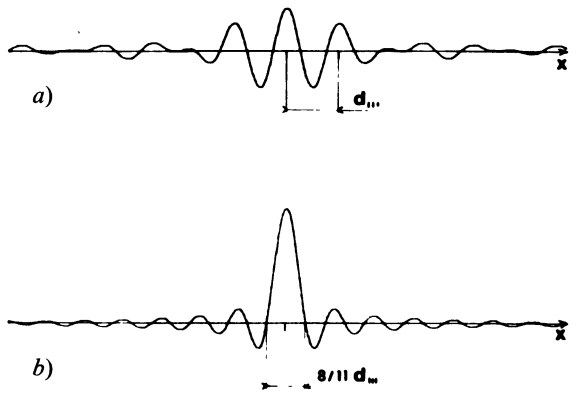

Fig. 6. — Amplitude of the inverse Fourier transform of the masks (in one dimension) : *a*) with three windows of width $2\, g_F = g_{111}/2$; *b*) with a window of width $2\, g_c = \frac{11}{4} g_{111}$; $d_{111} = 1/g_{111}$.

If the filter has a disc shape or is almost annular, the $h(x)$ function is narrower than the one given by holes, and has no important subsidiary maximum at the place of $1/g_{111}$. In fact the inverse Fourier transform of the disc filter is

$$h(x) = 2\, g_c \frac{\sin 2\pi g_c\, x}{2\pi g_c\, x}$$

where g_c is the cut off frequency $g_c = \frac{11}{8} g_{111}$ (Fig. 6*b*).

These remarks are of great consequence on the image reconstruction of the dislocation cores where the exact periodicity vanishes. If we use a filter with holes it is impossible to say if there is an atomic column or not, because of the presence of the parasitic spot due to the enhancement of the crystal periodicity. But the use of a ring and *a fortiori* a disc allows one to distinguish between the two core structures.

It may be noted that the disc case corresponds to the high resolution electron microscopy. Apart from the dynamical or geometrical imaging conditions we see that a *good* electron micrograph contains all the information about the core structure. Thus optical filtering with an almost annular mask should be used to improve the contrast and the signal to noise ratio. The information about the core of the dislocation is not concentrated just around the diffraction spot. Thus the annular mask shape is optimal. It removes a part of noise but transfers enough information on the core.

5. **Numerical filtering.** — 5.1 NUMERICAL FILTERING OF THE TEST OBJECTS. — A. Renault simulated numerically two dislocation cores similar to those described in 3.1 [19], he then computed the Fourier components of the 128 × 128 digitized object and then applied two different numerical masks : a mask with holes as in figure 4*b* and a disc mask as in figure 4*a*.

The conclusions are in agreement with those obtained in paragraph 4.2 (Fig. 7). In particular, when a mask with holes surrounding the diffracted spots is used, a supplementary atomic column appears in both objects (Fig. 7*a*) in fact the use of a mask with holes enhances the averaging effect, that is, it enhances the selected periodicities. This is of interest for periodic objects but is disastrous for non periodic objects such as dislocation cores. If a disc mask is used the distinction between the two cores can be made (Fig. 7*b*).

In these computed simulated cases the crystal far from the dislocation is well restored apart from the fact that the two atomic columns, 1.4 Å apart, are confused due to the cut off frequency of the mask.

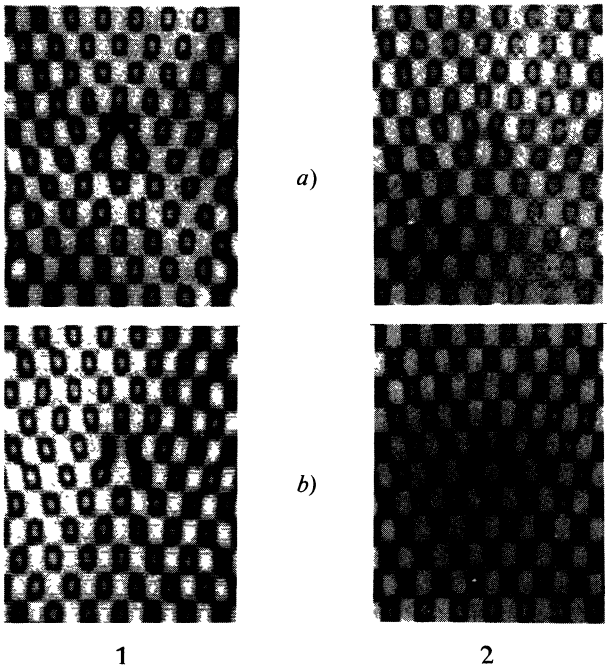

Fig. 7. — Numerical simulation of filtering of the two test objects (Fig. 2) with two mask shapes (5*a* and 5*b*) respectively 7*a* and 7*b* : (1) empty dislocation core ; (2) core with an atomic column.

5.2 NUMERICAL FILTERING OF AN ELECTRON MICROGRAPH. — We have tried to apply numerical filtering to the image of atomic columns around dislocations of the type described in 3.1. The micrograph was recorded at 500 kV. There were 8 identical dislocations located along a subgrain boundary [17]. The eight magnified images were superimposed. All the original dislocations have a white dot (positive print) at the core. It makes the superimposing easier. We then have to filter the resulting image.

The image is digitized on a 128 × 128 grid (Fig. 8*a*). The average density value is subtracted. The central spot of the Fourier series is set to zero, so that the other weak spectral components will be more accurate. The 128 × 128 image is then surrounded with zero values to build a 256 × 256 image. This is effectively an interpolation in the frequency space and permits a greater accuracy on the position of the frequencies to be analysed.

Great care must be taken with the numerical Fourier analysis of periodic objects [20].

It gives the components of Fourier series whose fundamental sampling frequency is the inverse of the total length of the signal (in one dimension). If the signal contains frequencies which are not a multiple of this frequency or if the length of the limited sampled signal is not a complete period of the continuous signal, then spurious values appear in the Fourier components. These must not be confused with frequencies coming from a defect in the periodic object.

We filtered the two-dimensional Fourier series of our pseudo-periodic object with an annular mask (Fig. 8*b*, *c*). The reconstructed image is given figure 8*d*. The result is the amplitude distribution of the inverse Fourier series. The phase image variation is negligible. We see that the low and high frequency noise has been removed. The core of the dislocation always appears as a large white dot in a positive print. The restored micrograph is easier to interpret : the localization of the white dots becomes more accurate.

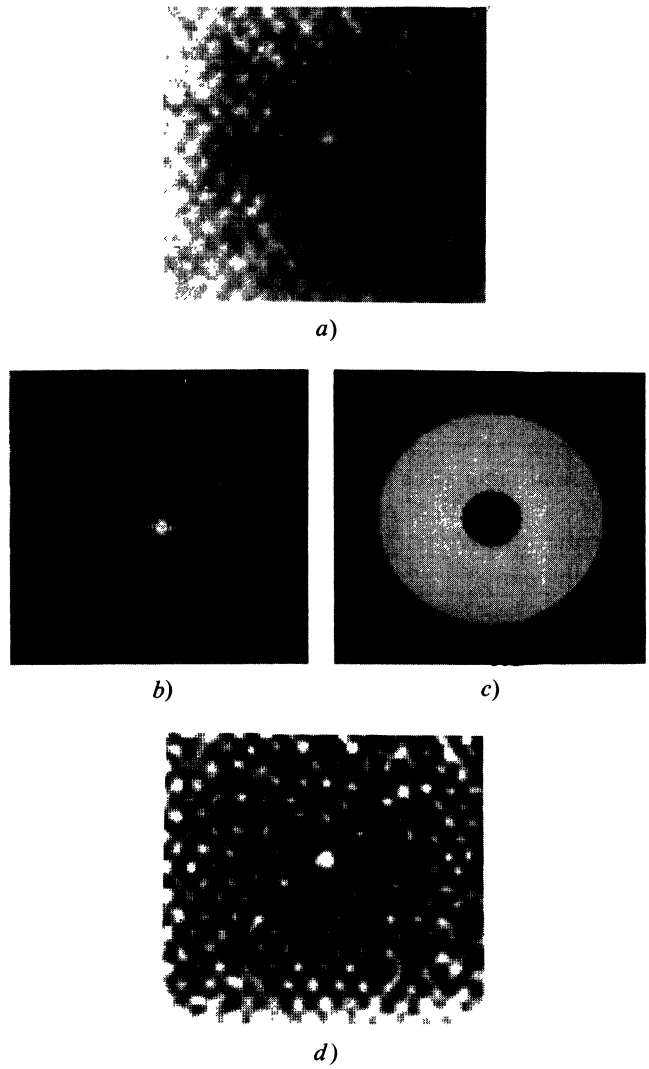

Fig. 8. — Numerical treatment of an electron micrograph of a dislocation core in Ge (011). 500 kV : *a*) original digitized micrograph ; *b*) Fourier transform amplitude ; *c*) annular mask used to suppress noise outside the frequency band $g_{MAX} = 1.4\ g_{111}$, $g_{MIN} = 0.4\ g_{111}$; *d*) restored image.

6. **Conclusion.** — Optical and numerical filtering processes are very attractive but great care must be taken so that neither artefacts nor lost of useful information may be produced.

In the ideal imaging conditions (high resolution high voltage microscopy at Scherzer focus) the transfer function has no sign reversal over a large frequency band and filtered images can be directly interpreted. But with 100 kV electron micrographs a full interpretation requires correction of the electron microscope aberrations and the exact dynamical conditions must be taken into account. Filtering permits us to reconstruct more useful images.

Acknowledgment. — The authors would like to thank Dick Wade for his friendly advice.

References

[1] VALENTINE, *Adv. in Optical and Electron Microscopy* (Acad. Press) 1966.
[2] SAJOVI, J., *Microsc. Spect. Elect.* (1979) accepted.
[3] THON, F., SIEGEL, B. M., *Ber. Buns. Ges.* **4** (1970) 1116.
[4] DESSEAUX, J., Doct. Thesis (1977), Grenoble.
[5] BOURRET, A., DESSEAUX, J., *Philos. Mag.* **2** (1977) 13.
[6] DESSEAUX, J., D'ANTERROCHES, D., PENISSON, J. M., RENAULT, A., 9th Int. Congress on Electron Microscopy, Toronto 1978, vol. **1**, p. 310.
[7] MARECHAL, A., CROCE, P., *C.R. Hebd. Séan. Acad. Sci.* **127** (1953) 607.
[8] KLUG, A., BERGER, J. E., *J. Mol. Biol.* **10** (1964) 565.

[9] KLUG, A., DE ROSIER, *Nature* **212** (1966) 29.
[10] O'NEIL, E., *IRE Trans. of Information Theory* **IT 2** (1956) 56.
[11] VAN DER LUGT, A., *Proc. IEEE* **54** (1966) 1055, *Opt. Acta* **15** (1968) 1, *Proc. IEEE* **62** (1974).
[12] GOODMAN, J., *Introduction to Fourier Optics* (Mac Graw-Hill) 1968.
[13] HIRTH, J., LOTHE, J., *Theory of dislocations* (Mac Graw-Hill) 1968.
[14] DONELLI, G., PAOLETTI, L., *Adv. Electron. Electron Phys.* **43** (1977) 1.
[15] TAYLOR, C. A., RANNIKO, J. K., *J. Microsc.* **100** (1974) 307.
[16] DESSEAUX, J., RENAULT, A., BOURRET, A., *Philos. Mag.* **35** (1977) 357.
[17] BOURRET, A., DESSEAUX, J., *Philos. Mag.* **39** (1979) 405.
[18] WILLIS, B. T. M., *Proc. R. Soc.* **A 239** (1957) 192.
[19] BOURRET, A., DESSEAUX, J., RENAULT, A., *J. Microsc. Spect. Elect.* **2** (1977) 467.
[20] HARRIS, F., *Proc. IEEE* **66** (1966) 51.